SPECIAL ISSUE ARTICLE

Filtering of Defects in Semipolar (11−22) GaN Using 2-Steps Lateral Epitaxial Overgrowth

N. Kriouche · M. Leroux · P. Vennéguès ·
M. Nemoz · G. Nataf · P. de Mierry

Abstract Good-quality (11−22) semipolar GaN sample was obtained using epitaxial lateral overgrowth. The growth conditions were chosen to enhance the growth rate along the [0001] inclined direction. Thus, the coalescence boundaries stop the propagation of basal stacking faults. The faults filtering and the improvement of the crystalline quality were attested by transmission electron microscopy and low temperature photoluminescence. The temperature dependence of the luminescence polarization under normal incidence was also studied.

Keywords Semipolar GaN · Epitaxial lateral overgrowth · TEM · Photoluminescence · Polarization

Introduction

Hexagonal III nitrides grown along the [0001] c-axis exhibit spontaneous and strain-induced polarizations [1]. The polarization-induced fields are detrimental in light-emitting diodes as they result in a spatial separation of electrons and holes on each side of the quantum wells, thus decreasing the radiative transition probability. This effect is known as the quantum-confined Stark effect (QCSE) [2]. To minimize this effect, heterostructures can be grown along a direction different from the c-axis. In particular, the (11−22) semipolar orientation can potentially suppress the internal electric fields [3]. In that case, the c-axis is inclined by 32.4° with respect to the surface.

In this paper, (11−22) oriented GaN films have been grown on m-plane (1−100) sapphire substrates, by metal-organic vapor-phase epitaxy (MOVPE). These films usually exhibit a huge density of structural defects, mainly stacking faults in inclined basal c-planes, i.e. basal stacking faults (BSFs) [4]. These BSFs are either terminated by partial dislocations (PDs) or connected to adjacent BSFs by stacking faults situated in prismatic planes (PSFs). The densities of BSFs, PDs and PSFs are in the 10^5 cm^{-1}, 10^{10} cm^{-2} and 10^3 cm^{-1} ranges, respectively [4]. Perfect threading dislocations (10^8 cm^{-2}) are also present. An alternative growth technique to get low defects density films is the Epitaxial Lateral Overgrowth (ELO). ELO has proven its effectiveness in defects reduction in c-plane GaN [5] and has also been applied for (11−22) semipolar orientations [6]. In this method, a dielectric mask pattern is deposited on a GaN layer by conventional photolithography processes. During a second epitaxy, the nucleation occurs selectively at the GaN openings between the dielectric stripes. These germs can then expand laterally above the stripes until coalescence and the formation of a bidimensional layer. The defect density above the GaN openings is identical to that of the GaN underlayer, whereas above the dielectric, it is strongly reduced. We previously had reported that the BSFs coming from the overgrowth above the mask openings could be efficiently eliminated, by using an asymmetric ELO process [7]. In this work, we summarize the different steps of the asymmetric ELO and confirm the filtering of BSFs using transmission electron microscopy. The improved optical quality of these semipolar ELO films allowed us to perform a detailed photoluminescence analysis as a function of temperature and light polarization.

N. Kriouche (✉) · M. Leroux · P. Vennéguès · M. Nemoz · G. Nataf · P. de Mierry
Centre de Recherche sur l'Hétéroépitaxie et ses Applications CRHEA-CNRS, Rue Bernard Grégory, Sophia Antipolis, 06560 Valbonne, France
e-mail: nk@crhea.cnrs.fr

Experiment

A 100-nm-thick SiO_2 film was deposited on a $(11-22)$ semipolar GaN on m-plane sapphire by RF sputtering. SiO_2 stripes of 7 μm width with a 3-μm spacing were patterned by conventional UV-lithography and chemical etching in a buffered oxide solution. The SiO_2 stripes were oriented parallel to the $[1-100]$ GaN m-axis. The ELO was performed in a home-made vertical MOVPE. Trimethylgallium and ammonia were used as precursors in a mixture of H_2/N_2 gas flows. The temperature was kept at 1,080°C during the entire process. A GaN crystal seed above the windows was first deposited at 20 kPa using a high V/III ratio ($\sim$ 3,500). In a second step, the pressure is decreased to 10 kPa and the V/III ratio was drastically reduced down to 500. Growth was pursued until full coalescence of the films.

TEM cross-sectional specimens were prepared by conventional mechanical and ion milling techniques, and the observations were carried out with a JEOL 2010F microscope operating at 200 kV. PL measurements were taken using the 244-nm line of a frequency-doubled argon laser. The polarized luminescence is collected by using a linear polariser placed between the sample and the monochromator.

Results and Discussion

ELO

The different steps of the asymmetric ELO are described in Fig. 1. Growth from the underlying GaN template above the openings leads, under appropriate MOVPE conditions, to the formation of crystals with an asymmetric shape.

The growth conditions enhance the growth rate along the $+c$ direction so that the $+c$ facets tend to disappear and the surface of the a facets increases. The crystal seeds therefore expand laterally until covering the a-facets of the adjacent crystal, as seen in Fig. 1a. Continuing the growth results in the formation of a fully coalesced layer (Fig. 1b). This process is thought to stop the propagation of BSFs at the coalescence boundary. The thin parallel lines in Fig. 1c represent the BSFs, inclined by 32° from the growth direction, originating from the template above the openings. The BSFs terminate in the coalescence boundary between two adjacent crystals. TEM experiments have been performed to verify this assumption.

Figure 2a, b is the cross-sectional TEM images of the coalescence boundaries along the $[2-1-10]$ zone axis. This orientation is inclined by 30° from the in-plane $[1-100]$ orientation and allows observing the stacking faults. BSFs are observable only on the $<1-100>$ dark field image (a) and are out of contrast in the (0002) dark field (b). On the other hand, PDs are observable on both images. Few BSFs are present on the—c-wings but these faults do not affect the final quality of the film because they are stopped by the adjacent crystal. The dotted arrows show the coalescence boundary, the upper left side of these images corresponding to a $+c$-laterally grown wing and the lower right side to a seed crystal. No faults are present above the coalescence boundary, neither PDs nor BSFs. These observations show that the overgrowth of a-facets by $+c$-laterally growing wings is a very efficient mechanism to avoid the propagation of BSFs and related defects to the surface of the coalesced films.
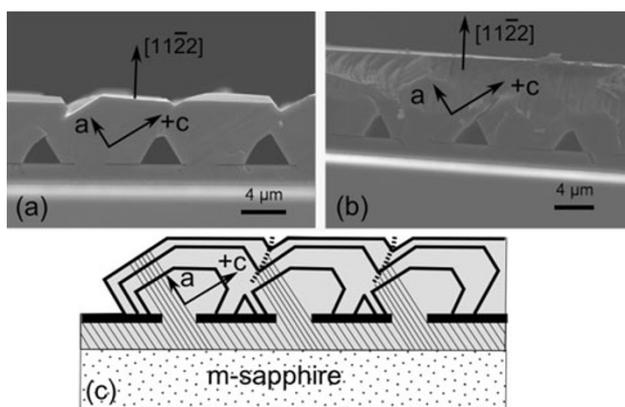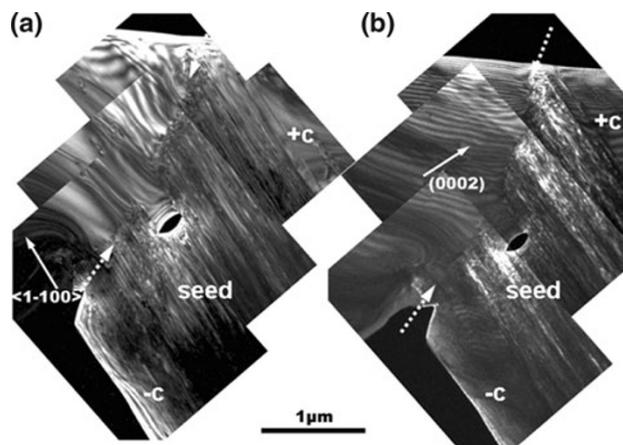

Fig. 1 Cross-sectional SEM images of **a** the GaN crystals at an intermediate growth stage, **b** after full coalescence. **c** Schematic representation of the crystal growth during asymmetric ELO. The lines inclined at 32° from the surface represent the BSFs. The a and $+c$ numbers refer to the crystallographic directions $[11-20]$ and $[0001]$, respectively

Fig. 2 Dark field TEM images of the coalescence boundary taken near the $[2-1-10]$ GaN zone axis with diffraction vectors along $[1-100]$ (**a**) and in the c-plane (**b**)
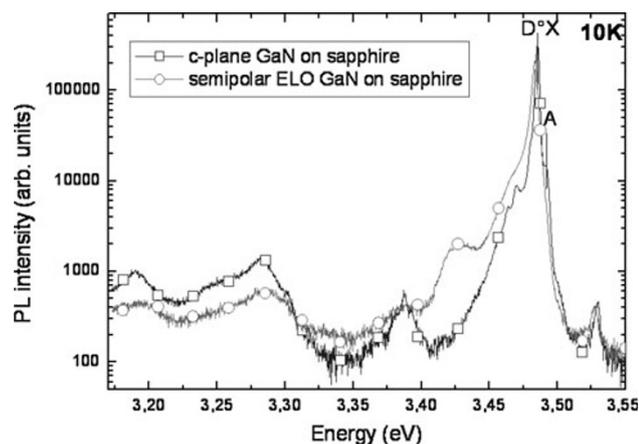
Fig. 3 Photoluminescence of asymmetric ELO sample and standard *c*-plane GaN template at 10 K

Photoluminescence

Figure 3 compares the luminescence of a standard *c*-plane GaN on sapphire sample with our semipolar asymmetric ELO sample at low temperature. The spectrum of the ELO sample is dominated by band edge transitions assigned to the donor-bound exciton D^0X and free *A* exciton recombinations 7 meV higher (3.485 and 3.492 eV, respectively). The intensity of the band edge emission is comparable to that of a standard *c*-plane GaN with a dislocations density of $\sim 5 \times 10^8$ cm^{-2}. Very weak emission at 3.42 eV is ascribed to the luminescence of excitons bound to BSFs. The intensity ratio between band edge and BSF luminescence is about 100, confirming that asymmetric ELO has efficiently filtered most of the BSFs. The luminescence at 3.28 eV corresponds to donor–acceptor (D^0A^0) transitions.

The luminescence of the semipolar asymmetric ELO sample was studied as a function of temperature and light polarization. Figure 4a shows the evolution of the PL intensity with the temperature of the band edge (D^0X and *A* exciton) and the D^0A^0 transitions. The inset shows the

geometry of the experiment, the growth axis being the *x*-axis. Two different linear polarizations were collected. One being perpendicular to the stripes (**E** $\perp$ *m*) and the other one parallel to the stripes (**E** $\parallel$ *m*), where m is the [1–100] direction. The intensities decrease with increasing temperature, due to the thermal activation of non-radiative centers. These evolutions can be fitted using one or two thermally activated non-radiative recombination channels (dotted lines) [8]:

$$I = \frac{I_0}{1 + a\exp\left(\frac{E_1}{kT}\right)} \tag{1}$$

$$I = \frac{I_0}{1 + a\exp\left(\frac{E_1}{kT}\right) + b\exp\left(\frac{E_2}{kT}\right)}. \tag{2}$$

The fitting of the D^0A^0 band is done by the Eq. 1. The activation energy for the two polarizations is 170 meV. This corresponds to hole released from the acceptors, as already observed for heteroepitaxial *c*-plane GaN [8]. For **E** $\perp$ *m*, the band edge emission is fitted using the same equation until 100 K, with $E_1 = 5.5$ meV, the binding energy of excitons to the donor. Beyond 100 K, the PL intensity slightly increases, because of acceptors ionization and the increase in the B exciton population. For **E** $\parallel$ m, the band edge exciton intensity is fitted using Eq. 2 with an activation energy E_1 of 6.5 and 100 meV for the second activation energy. The origin of this second activation energy is not clear.

Figure 4b shows the evolution of the ratio of intensities measured for light polarized along and perpendicular to m ($I_\parallel/I_\perp$). In *relaxed* GaN, the ground state exciton (*A* exciton) symmetries are Γ_6 (forbidden) and Γ_5, which is allowed but does not couple with the component of the electric field parallel to the *c*-axis. As such, the intensity ratio $I_\parallel/I_\perp$ for relaxed GaN is expected to be $1/\sin^2\theta$, with $\theta = 90 - \mathrm{tg}^{-1}[(c/n)/(a/2)]$ for (11–2n) planes (*c* and *a* are the lattice parameters). For the (11–22) plane, $\theta = 32.6°$ and $1/\sin^2\theta = 3.45$. However, whatever the transition

Fig. 4 a Intensities evolution with temperature of band edge and $D°A°$ transition for light polarized along and perpendicular to *m*-axis and **b** intensity ratio of band edge and $D°A°$ transitions between the two polarizations as a function of temperature
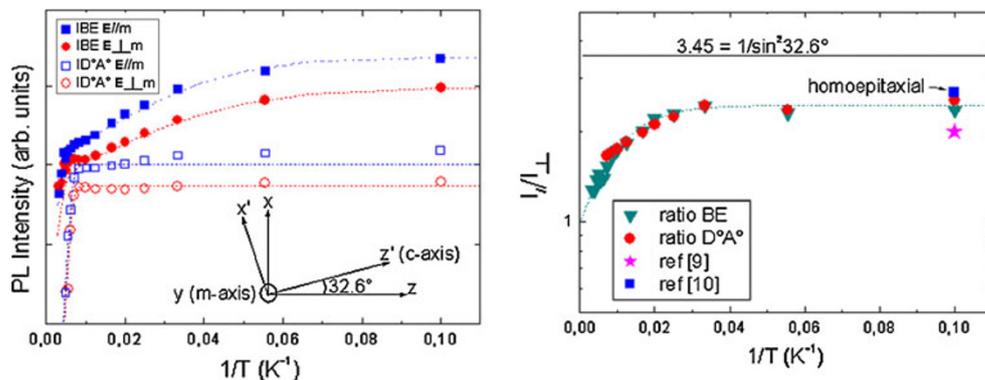
band edge or D^0A^0, the ratio is equal to ~ 2.3 at low temperature. This value must be compared with the ratio of 2 found by Gühne et al. [9] for standard $(11-22)$ ELO semipolar GaN on sapphire and the ratio of 2.7 for $(11-22)$ homoepitaxial GaN [10]. The measured values are always lower than 3.45. Moreover, the values found for hetero-epitaxial samples are lower than that found for homoepit-axial sample. In fact, the symmetry of heteroepitaxial semipolar ELO GaN films is lower than the wurtzite one, due to anisotropic strains. This decrease in the symmetry implies a splitting of energy levels and increases the oscillator strength of A excitons along the c-axis and so along z [9]. This explains the lower intensity ratio than in the case of the wurtzite symmetry. This intensity ratio decreases when the temperature rises, following Eq. 1 [9] with an activation energy $E_1 \sim 11$ meV. This decrease is due to the populating of B excitons, whose oscillator strength is higher for $\mathbf{E} \perp m$. Note that the activation energy found from Fig. 4b is in good agreement with the $A–B$ splitting measured by reflectivity on similar samples [7]. When the temperature tends toward infinity, the intensity ratio tends to 1, as expected, since all levels are expected to be equally populated.

Conclusions

The ELO process at low pressure and low V/III ratio enhances the $+c$ facet growth rate, and the propagation of stacking faults is stopped at the coalescence boundaries. The filtering efficiency is shown in the cross-sectional TEM images. The good quality of the sample is also seen by low-temperature photoluminescence, displaying high band edge emission intensity, which is comparable to that of standard c-plane GaN on sapphire, and a low BSFs-related emission intensity. The study of photoluminescence as a function of temperature and light polarization allows to highlight a decrease in the symmetry of semipolar ELO GaN and so an anisotropic strain.

References

1. F. Bernardini, V. Fiorentini, D. Vanderbilt, Phys. Rev. B. **56**, R10024 (1997)
2. D.A.B. Miller, D.S. Chemla, T.C. Damen, A.C. Gossard, W. Wiegmann, T.H. Wood, C.A. Burrus, Phys. Rev. Lett. **53**, 2173 (1984)
3. A.E. Romanov, T.J. Baker, S. Nakamura, J.S. Speck, J. Appl. Phys. **100**, 023522 (2006)
4. P. Vennéguès, Z. Bougrioua, T. Gühne, Jpn. J. Appl. Phys. **46**, 4089 (2007)
5. P. Gibart, Rep. Prog. Phys. **67**, 667–715 (2004)
6. T. Guehne, Z. Bougrioua, P. Vennéguès, M. Leroux, M. Albrecht, J. Appl. Phys. **101**, 113101 (2007)
7. P. de Mierry, N. Kriouche, M. Nemoz, G. Nataf, Appl. Phys. Lett. **94**, 191903 (2009)
8. M. Leroux, N. Grandjean, B. Beaumont, G. Nataf, F. Semond, J. Massies, P. Gibard, J. Appl. Phys. **86**, 3721 (1999)
9. T. Gühne, Z. Bougrioua, S. Laüt, M. Nemoz, P. Vennéguès, B. Vinter, M. Leroux, Phys. Rev. B **77**, 075308 (2008)
10. M. Ueda, K. Kojima, M. Funato, Y. Kawakami, Appl. Phys. Lett. **89**, 211907 (2006)